

# Förster resonance energy transfer-based total internal reflection fluorescence reader for apoptosis

## Thomas Bruns

Hochschule Aalen  
Institut für Angewandte Forschung  
Beethovenstrasse 1  
73430 Aalen, Germany

## Brigitte Angres

## Heiko Steuer

NMI Naturwissenschaftliches und Medizinisches  
Institut an der Universität Tübingen  
Markwiesenstr. 55  
72770 Reutlingen, Germany

## Petra Weber

## Michael Wagner

## Herbert Schneckenburger

Hochschule Aalen  
Institut für Angewandte Forschung  
Beethovenstrasse 1  
73430 Aalen, Germany

**Abstract.** A fluorescence reader for the detection of Förster resonance energy transfer (FRET) on surfaces of living cells is described. The method is based on multiple total internal reflections (TIR) of an incident laser beam within a glass slide, such that individual samples on top of the glass slide are illuminated simultaneously by an evanescent electromagnetic field. Enhanced cyan fluorescent protein (ECFP) anchored to the inner leaflet of the plasma membrane is optically excited and transfers its excitation energy via the peptide linker Asp-Glu-Val-Asp (DEVD) to an enhanced yellow fluorescent protein. Upon apoptosis, DEVD is cleaved, and energy transfer is disrupted, as proven by an increase of fluorescence intensity as well as of fluorescence lifetime of the donor ECFP. Due to selective excitation of membrane-associated fluorophores, intracellular fluorescence and background luminescence from the surrounding medium are eliminated. Therefore, this test system appears to be a sensitive device for the detection of apoptosis and more generally for drug screening or *in vitro* diagnosis on a nanometer scale. © 2009 Society of Photo-Optical Instrumentation Engineers. [DOI: 10.1117/1.3055622]

Keywords: cells; membranes; apoptosis; fluorescence reader; total internal reflection; fluorescence lifetime; FRET.

Paper 082745SR received Aug. 7, 2008; revised manuscript received Oct. 8, 2008; accepted for publication Oct. 8, 2008; published online Mar. 4, 2009.

## 1 Introduction

Resonant transfer of optical excitation energy via dipole-dipole interaction was described by Förster about 60 years ago.<sup>1</sup> Although this kind of energy transfer is well known in nature (e.g., in plants where optically excited antenna molecules transfer their energy to the reaction centers<sup>2</sup>), it was not used in cell biology and biotechnology until the 1980s.<sup>3-5</sup> After successful cloning of the gene encoding for green fluorescent protein (naturally produced by the jellyfish *Aequorea Victoria*)<sup>6</sup> and its variants emitting light in the blue, yellow, or red spectral ranges, Förster resonance energy transfer (FRET) from an optically excited donor to an acceptor molecule has become a well-established and broadly used analytical technique. This technique has also been applied for the detection of programmed cell death (apoptosis) by fusing cyan fluorescent protein (CFP) to yellow fluorescent protein (YFP) with a caspase-3 sensitive peptide Asp-Glu-Val-Asp (DEVD) used as a linker.<sup>7,8</sup> Upon induction of apoptosis, this linker was cleaved by caspase-3 activity, and FRET was interrupted. So far, FRET has been deduced from stationary measurements of donor (CFP) and acceptor (YFP) fluorescence, and a decrease of its efficiency up to a factor of five has been calculated.<sup>9</sup> In view of further enhancement of FRET sensitivity as well as suppression of background fluorescence, enhanced CFP (ECFP) was anchored to the plasma membrane of HeLa cer-

vical carcinoma cells, as depicted in Fig. 1, and membrane-associated fluorescence was excited selectively by an evanescent electromagnetic field.<sup>10</sup> Energy transfer from donor (ECFP) to acceptor (enhanced YFP, EYFP) molecules was deduced from the ratio of acceptor/donor fluorescence as well as from the fluorescence lifetime of the donor, which, according to the equation

$$1/\tau - 1/\tau_0 = k_{ET}, \quad (1)$$

permits the calculation of the energy-transfer rate  $k_{ET}$  ( $\tau$ ,  $\tau_0$  = fluorescence lifetimes in the presence and absence of the acceptor, respectively).

Thus,  $k_{ET}$  has been determined from measurements of individual cells, where apoptosis could be visualized by cell morphology. In contrast, larger cell collectives without any visual control were used in the present paper, i.e., mixed populations of apoptotic and nonapoptotic cells were examined, and apoptosis (of part of the cells) was deduced from changes in fluorescence lifetimes and intensities of the donor ECFP. In view of potential applications in high-content screening it was a main purpose of this paper to excite a larger number of individual samples simultaneously upon total internal reflection (TIR) of an incident laser beam with a penetration depth of the evanescent electromagnetic field around 100–150 nm. Therefore, an existing TIR reader system with multiple TIRs up to 96 individual wells of a microtiter plate<sup>11</sup> was modified for FRET measurements.

Address all correspondence to Herbert Schneckenburger, Hochschule Aalen, Institut für Angewandte Forschung, Beethovenstr. 1, 73430 Aalen, Germany. Tel.: +49 7361 576 3401; Fax: +49 7361 576 3318; E-mail: herbert.schneckenburger@htw-aalen.de

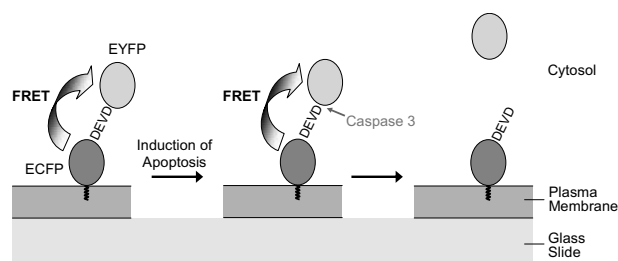


**Fig. 1** Membrane-associated test system for apoptosis based on FRET and its interruption.

## 2 Materials and Methods

### 2.1 Plasmid Construction

A membrane-bound caspase-3-sensitive FRET probe was generated that contains the DEVD linker sequence described by Nagai and Miyawaki<sup>12</sup> for the SCAT3.1 construct. In brief, using standard polymerase chain reaction (PCR) techniques and the plasmids pECFP-Mem and pEYFP-C1 (both from BD Biosciences Clontech, Palo Alto, CA) as templates, two PCR fragments were generated and fused to yield cDNA, encoding the N-terminal signal sequence for post-translational palmitoylation, followed by ECFP linked to EYFP by the SCAT3.1 DEVD sequence. This cDNA was cloned into the backbone of the vector pMemECFP to yield the plasmid MemECFP-DEVD-EYFP. A similar construct was generated containing the noncleavable sequence Asp-Glu-Val-Gly (DEVG) instead of DEVD for control experiments (MemECFP-DEVG-EYFP). The same plasmids were also used in the work of Angres et al.<sup>10</sup>

### 2.2 Cell Culture and Cell Incubation

HeLa cervical carcinoma cells were grown at 37°C, 5% CO<sub>2</sub>, in minimum essential medium (MEM) growth medium containing MEM medium supplemented with 10% fetal calf serum, nonessential amino acids, 100 U/mL penicillin, 100 ng/mL streptomycin, and 2 mM glutamine. Transient cell transfections with plasmids were performed by lipofection using the FuGene transfection kit (Roche, Mannheim, Germany) according to the manufacturer's instructions. For the establishment of stable cell lines, HeLa cells were grown in six well plates up to 90% confluency at 37°C, 5% CO<sub>2</sub>, and 90% humidity in MEM growth medium. Transfection was performed by lipofection with FuGene according to the manufacturer's instructions with a ratio of 3 μL FuGene HD per 1 μg DNA using 1, 2, or 4 μg/well of plasmids MemECFP-DEVD-EYFP or MemECFP-DEVG-EYFP. After 24 h, the medium was exchanged for MEM growth medium supplemented with 400 μg/mL G418. After 4–5 weeks of selection and expansion, fluorescent single cells were sorted into 96 well plates via a FACSaria cell-sorting system (BD Biosciences, USA) in conditioned MEM growth medium gained from a one day HeLa cell culture. Stable clones were subsequently raised in MEM growth medium supplemented with 200 μg/mL G418.

For all experiments on the TIR Reader, stable cell lines expressing either MemECFP-DEVD-EYFP or MemECFP-DEVG-EYFP were used. Cells were seeded at a density of 500 cells/mm<sup>2</sup> within specific cavities on glass slides (see

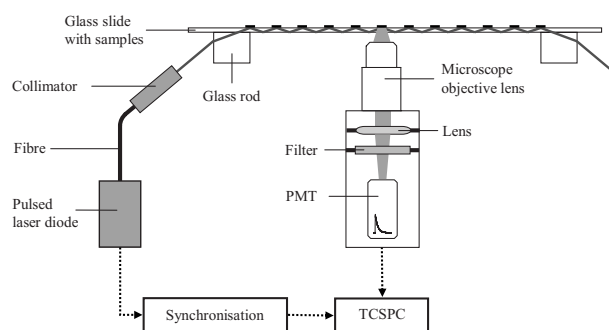


**Fig. 2** TIR fluorescence-lifetime reader (TCSPC=Time-correlated single-photon counting).

below). After a growth phase of 48 h (to obtain a subconfluent monolayer), cells were incubated for 4 h with 2 μM staurosporine (S6942, Sigma-Aldrich Chemie GmbH, Germany) diluted in cultivation medium in order to induce apoptosis. Fluorescence of all samples was measured before and after incubation with staurosporine.

### 2.3 TIR Reader

For excitation of the membrane-associated donor ECFP or for direct excitation of the acceptor EYFP, we used pulsed laser diodes (pulse duration: 50–70 ps, repetition rate: up to 40 MHz, LDH-P-C-400 or LDH-P-C-470 with driver PDL 800-B, PicoQuant GmbH, Berlin, Germany) emitting light at 391 nm (average power: 65 μW) or 470 nm (average power: 100 μW), respectively. Collimated laser beams were coupled into a conventional microscope glass slide of 1 mm thickness (with superimposed cavities for individual samples) via polarization, maintaining single-mode fibers (kineFlex, Point Source, Southampton, UK) and a glass rod of rectangular shape, as depicted in Fig. 2. In all cases, the electric-field vector was polarized perpendicular to the plane of incidence. Multiple TIRs occurred within the glass slide if the angle of incidence  $\Theta$  was above the critical angle  $\Theta_c=63.9$  deg (resulting from the refractive indices  $n_1=1.525$  for the glass bottom and  $n_2=1.37$  for the cells). In the present setup, an angle  $\Theta=66$  deg was chosen, resulting in a distance  $s=4.5$  mm between individual samples and a penetration depth  $d=120$ – $150$  nm of the evanescent electromagnetic wave within the cells (depending on the excitation wavelength) according to

$$d = (\lambda/4\pi)(n_1^2 \sin^2 \Theta - n_2^2)^{-1/2}. \quad (2)$$

Due to the Gaussian-shaped laser-beam profile of 500 μm diam, each illumination spot on up to 12 samples (of about 1000 cells each) was of elliptical shape with an area around 0.5 mm<sup>2</sup>. At the end of the glass slide, laser light was coupled with a second glass rod to avoid uncontrolled reflections.

Fluorescence intensities of all samples were detected simultaneously by an integrating digital charge-coupled device (CCD) camera (ProgRes C10, Jenoptik GmbH, Germany) equipped with a wide-angular objective lens (Cinegon 1.4/12–0515, Schneider GmbH, Germany). ECFP fluorescence (excited at 391 nm) was measured with a bandpass filter at 475 ± 20 nm, whereas EYFP fluorescence (excited

directly at 470 nm) was detected with a long pass filter at  $\lambda \geq 515$  nm. Exposure times were 10 s at 470 nm and 20 s at 391 nm. Measurements of EYFP fluorescence at an excitation wavelength of 391 nm (ECFP excitation with subsequent energy transfer ECFP  $\rightarrow$  EYFP) were omitted, because in this case a spectral overlap by ECFP was unavoidable. After measurement of fluorescence intensities<sup>11</sup> prior to ( $I_p$ ) and after ( $I_a$ ) incubation with staurosporine, the ratio  $I_a/I_p$  of all samples was calculated, and median values  $\pm$  median absolute deviations (MADs) of this ratio were determined for 20–30 individual measurements of HeLa-MemECFP-DEVD-EYFP as well as HeLa-MemECFP-DEVG-EYFP cells. Control measurements were carried out with cells prior to and after a time interval of 4 h but without application of staurosporine. Because of possible errors due to light absorption in the glass slide, variations in the number of cells per sample or optical aberrations within the detection path affected  $I_a$  and  $I_p$  in the same way, these errors were eliminated by calculation of the ratio  $I_a/I_p$ . Therefore, no further correction was needed.

In addition to fluorescence intensities, we determined fluorescence lifetimes of ECFP using the same optical setup as reported above with the following changes: the repetition rate of the 391 nm laser diode was reduced to 20 MHz, and the CCD camera was replaced by a microscope objective lens ( $20\times/0.50$ ), a photomultiplier tube (H5783-01, Hamamatsu Photonics Deutschland GmbH, Germany), and a time-correlated single-photon counting device (TimeHarp 200, PicoQuant GmbH, Berlin, Germany), as depicted in Fig. 2. Because in this case simultaneous measurements of all samples were not possible, the whole detection unit was moved on a programmable scanning table and positioned below each sample of interest. Fluorescence decay curves  $I(t)$  were fitted as a sum of exponential terms corresponding to

$$I(t) = \sum_i A_i \exp^{-t/\tau_i} \quad (3)$$

with fluorescence lifetimes  $\tau_i$  and pre-exponential factors  $A_i$  representing the fractional contributions of the component  $i$ . The decay parameters were iteratively recovered with a non-linear least-squares error minimization based on the Levenberg–Marquardt algorithm.<sup>13</sup> The reduced  $\chi^2$  ratios and their autocorrelation functions were used to facilitate the assessment of the fit quality. A  $\chi^2$  value below 1.2 is regarded to be an indicator of a good fit.<sup>14</sup>

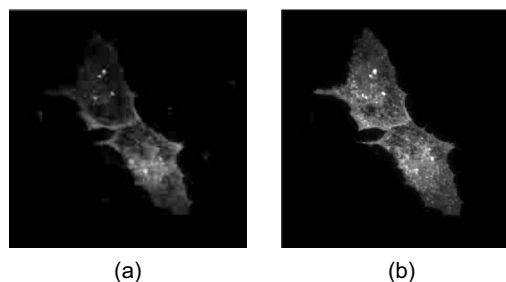


**Fig. 3** TIR images of HeLa cells transiently transfected with the MemECFP-DEVD-EYFP plasmid upon excitation of the donor (ECFP) at 391 nm and its detection at  $475 \pm 20$  nm (a) as well as upon excitation of the acceptor (EYFP) at 470 nm and its detection at  $\lambda \geq 515$  nm (b). Image size:  $140 \times 140 \mu\text{m}$ .

## 2.4 Microscopic Measurements

To visualize membrane-associated fluorescence of ECFP and EYFP in single cells, a fluorescence microscope (Axioplan 1, Carl Zeiss Jena, Germany) equipped with a TIR condenser (coupled to the laser diodes via single-mode fibers),<sup>15</sup> a  $40\times/1.30$  (oil) objective lens, and an electron-multiplying CCD camera<sup>16</sup> was used. The same system had already been used to measure fluorescence spectra and decay kinetics of individual cells.<sup>10</sup> Excitation wavelengths and spectral filtering were the same as mentioned above.

## 3 Results and Discussion

TIR images of HeLa-MemECFP-DEVD-EYFP cells under the fluorescence microscope are depicted in Fig. 3 upon optical excitation of donor (a) or acceptor (b) molecules. Donor fluorescence in Fig. 3(a) was selected by an interference filter at  $475 \pm 20$  nm, whereas acceptor fluorescence in Fig. 3(b) was measured exclusively at  $\lambda \geq 515$  nm. Similarity of both images proves colocalization of ECFP and EYFP molecules within the MemECFP-DEVD-EYFP complex.

Intensity ratios  $I_a/I_p$  of the donor ECFP in TIR reader experiments after ( $I_a$ ) and prior to ( $I_p$ ) the application of staurosporine are given in Table 1 for HeLa-MemECFP-DEVD-EYFP as well as for HeLa-MemECFP-DEVG-EYFP cells (the latter containing the noncleavable linker DEVG). This table shows that the intensity of ECFP fluorescence in HeLa-MemECFP-DEVD-EYFP cells increased upon apoptosis,

**Table 1** Intensity ratio of ECFP and EYFP fluorescence after ( $I_a$ ) and prior to ( $I_p$ ) incubation with staurosporine (4 h) in two transfected HeLa cell lines (medians  $\pm$  MADs). ECFP was excited at 391 nm and measured at  $475 \pm 20$  nm, whereas EYFP was excited at 470 nm and measured at  $\lambda \geq 515$  nm. In control experiments,  $I_a$  was also determined after 4 h but without staurosporine. The number of measurements is indicated in brackets.

	HeLa-MemECFP-DEVD-EYFP		HeLa-MemECFP-DEVG-EYFP	
	ECFP	EYFP	ECFP	EYFP
$I_a/I_p$	$1.1185 \pm 0.0395$ [30]	$0.7731 \pm 0.0384$ [20]	$0.9838 \pm 0.0267$ [20]	$0.6608 \pm 0.0616$ [20]
$I_a/I_p$ control	$0.9864 \pm 0.0179$ [30]	$0.9705 \pm 0.0170$ [20]	$0.9789 \pm 0.0138$ [20]	$0.8526 \pm 0.0263$ [20]

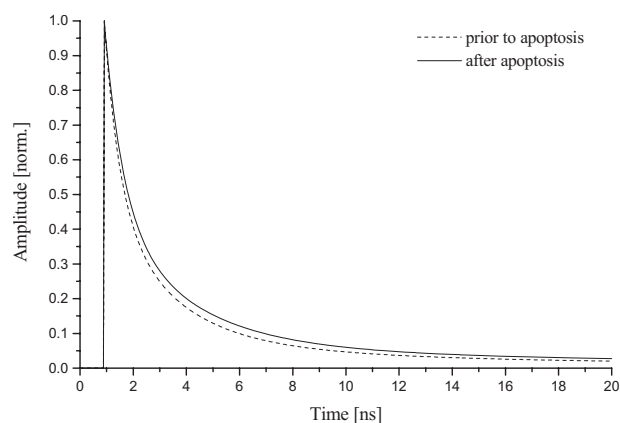


**Fig. 4** Fluorescence decay curves of ECFP in HeLa-MemECFP-DEVD-EYFP cells prior to and after application of staurosporine (individual samples). Excitation wavelength: 391 nm; detection range:  $475 \pm 20$  nm.

when energy transfer to EYFP was disrupted, but remained constant in HeLa-MemECFP-DEVG-EYFP cells as well as in control cells (without incubation with staurosporine). In contrast to ECFP, EYFP fluorescence decreased in HeLa-MemECFP-DEVD-EYFP as well as in HeLa-MemECFP-DEVG-EYFP cells. In the case of the DEVD construct, one would expect that this was due to cleavage of EYFP from ECFP and subsequent EYFP movement out of the evanescent field of illumination. However, EYFP decreased also in cells containing the DEVG control construct, where cleavage was not expected to occur<sup>10</sup> (and where, consequently, ECFP fluorescence did not increase). Looking for an explanation of this finding, we observed in microscopic experiments that part of the cells were detached from the surface upon incubation with staurosporine. Their escape from the surface upon incubation with staurosporine might be a dominating effect in the TIR reader for both cell lines and could explain a general decrease of fluorescence, which appeared to be more pronounced for EYFP than for ECFP. Evaluation of EYFP fluorescence may be fur-

ther complicated by some fluorescence fading observed in control measurements of HeLa-MemECFP-DEVG-EYFP cells (without incubation with staurosporine). Therefore, until now only the fluorescence intensity of MemECFP, but not that of EYFP, can be used as an indicator of apoptosis.

Decay curves of ECFP fluorescence in HeLa-MemECFP-DEVD-EYFP cells after picosecond laser pulse excitation are depicted in Fig. 4 prior to and after application of staurosporine. The fluorescence decrease appears slightly longer after incubation with staurosporine. This is confirmed by the median values  $\pm$  MADs of 21 individual experiments depicted in Table 2. All decay curves were fairly tri-exponential with fluorescence lifetimes around 0.65, 2.6, and 10.6 ns, relative amplitudes of about 0.52, 0.41, and 0.07, and  $\chi^2$  values around 1.15. Upon addition of staurosporine, almost no changes of relative amplitudes were observed, whereas all fluorescence lifetimes increased in HeLa-MemECFP-DEVD-EYFP and remained constant in HeLa-MemECFP-DEVG-EYFP cells. This indicates that according to Eq. (1), energy transfer was interrupted or lowered when the cleavable linker DEVD was used, but not when the noncleavable linker DEVG was used, and shows that apoptosis can be evaluated in principle on the basis of fluorescence lifetimes of a membrane-associated fluorescent protein (ECFP).

A prolongation of the fluorescence lifetime  $\tau_2$  of ECFP upon interruption of energy transfer ECFP  $\rightarrow$  EYFP has already been detected by fluorescence microscopy of individual apoptotic cells.<sup>10</sup> Because the induction of apoptosis by staurosporine after 4 h is never homogeneous in a cell population,<sup>17</sup> it should be emphasized that a similar prolongation is now measured for a mixed population of apoptotic and nonapoptotic cells without any visual control. This prolongation now includes the fluorescence lifetimes  $\tau_1$  and  $\tau_3$ , as depicted in Table 2 and predicted by Eq. (1). Only the two shorter components ( $\tau_1, \tau_2$ ), but not the comparably weak long-lived component ( $\tau_3$ ), can be correlated with literature data of (E)CFP fluorescence.<sup>18,19</sup>

Commonly, fluorescence readers in clinical and pharmaceutical laboratories include parallel detection of larger cell

**Table 2** Decay times, relevant amplitudes (normalized to 1), and  $\chi^2$  values of ECFP fluorescence after and prior to incubation with staurosporine (4 h) in two transfected HeLa cell lines (medians+MADs). ECFP was excited at 391 nm and measured at  $475 \pm 20$  nm. The number of measurements is indicated in brackets.

	HeLa-MemECFP-DEVD-EYFP		HeLa-MemECFP-DEVG-EYFP	
	prior to incubation	+2 $\mu$ M staurosporine	prior to incubation	+2 $\mu$ M staurosporine
$\tau_1$ [ns]	0.656 $\pm$ 0.018 [21]	0.684 $\pm$ 0.023 [21]	0.626 $\pm$ 0.036 [21]	0.623 $\pm$ 0.022 [21]
$\tau_2$ [ns]	2.626 $\pm$ 0.070 [21]	2.746 $\pm$ 0.056 [21]	2.617 $\pm$ 0.058 [21]	2.614 $\pm$ 0.041 [21]
$\tau_3$ [ns]	10.64 $\pm$ 0.30 [21]	11.43 $\pm$ 0.15 [21]	11.52 $\pm$ 0.46 [21]	11.17 $\pm$ 0.22 [21]
A <sub>1</sub> [norm.]	0.522 [21]	0.516 [21]	0.510 [21]	0.535 [21]
A <sub>2</sub> [norm.]	0.405 [21]	0.413 [21]	0.421 [21]	0.400 [21]
A <sub>3</sub> [norm.]	0.073 [21]	0.071 [21]	0.069 [21]	0.065 [21]
$\chi^2$	1.157 [21]	1.128 [21]	1.132 [21]	1.152 [21]

collectives in microtiter plates, e.g., for evaluation of drug effects on cells. Those plate readers have previously also been used for stationary measurements of FRET, including its application to apoptosis.<sup>20,21</sup> The main advantages of the present reader system over existing systems are the involvement of fluorescence-lifetime measurements as well as sample excitation by an evanescent electromagnetic field with multiple TIRs of an incident laser beam. This permits versatile measurements of membrane-associated fluorophores within nanometer ranges, offering perfect suppression of background fluorescence from inner parts of the cells as well as from the surrounding medium. Therefore, the present system appears to be a sensitive device not only for detection of apoptosis but, more generally, for drug screening and *in vitro* diagnostics in a nanometer scale.

### Acknowledgments

This project was funded by the Landesstiftung Baden-Württemberg GmbH. Technical assistance by Claudia Hintze is gratefully acknowledged. We thank the staff members of the Core Facilities of the Interdisziplinäres Zentrum für Klinische Forschung (IZKF) of the Universitätsklinikum Tübingen for conducting the cell sorting.

### References

1. T. Förster, "Zwischenmolekulare energiewanderung und fluoreszenz," *Ann. Phys. (N.Y.)* **2**, 57–75 (1948).
2. W. L. Butler, "Energy distribution in the photochemical apparatus of photosynthesis," *Annu. Rev. Plant Physiol.* **29**, 345–378 (1978).
3. D. L. Taylor, J. Reidler, A. Spudich, and L. Stryer, "Detection of actin assembly by fluorescence energy transfer," *J. Cell Biol.* **89**, 65–87 (1981).
4. P. S. Uster and R. E. Pagano, "Resonance energy transfer microscopy: observations of membrane-bound fluorescent probes in model membranes and in living cells," *J. Cell Biol.* **103**, 1221–1234 (1986).
5. J. Szöllösi, S. Damjanovich, S. A. Mulhern, and L. Tron, "Fluorescence energy transfer and membrane potential measurements monitor dynamic properties of cell membranes: a critical review," *Prog. Biophys. Mol. Biol.* **49**, 65–87 (1987).
6. C. W. Cody, D. C. Prasher, W. M. Westler, F. G. Prendergast, and W. Ward, "Chemical structure of the hexapeptide chromophore of the *Aequorea* green-fluorescent protein," *Biochemistry* **32**, 1212–1218 (1993).
7. X. Xu, A. L. Gerard, B. C. Huang, D. C. Anderson, D. G. Payan, and Y. Luo, "Detection of programmed cell death using fluorescence energy transfer," *Nucleic Acids Res.* **26**(8), 2034–2035 (1998).
8. N. P. Mahajan, D. C. Harrison-Shostak, J. Michaux, and B. Herman, "Novel mutant green fluorescent protein protease substrates reveal the activation of specific caspases during apoptosis," *Chem. Biol.* **6**(6), 401–409 (1999).
9. K. Q. Luo, V. C. Yu, Y. Pu, and D. C. Chang, "Application of the fluorescence resonance energy transfer method for studying the dynamics of caspase-3 activation during UV-induced apoptosis in living HeLa cells," *Biochem. Biophys. Res. Commun.* **283**(5), 1054–1060 (2001).
10. B. Angres, H. Steuer, P. Weber, M. Wagner, and H. Schneckenburger, "A membrane-bound FRET-based caspase sensor for detection of apoptosis using fluorescence lifetime and total internal reflection microscopy," *Cytometry Part A*, in press.
11. T. Bruns, W. S. L. Strauss, R. Sailer, M. Wagner, and H. Schneckenburger, "Total internal reflectance fluorescence reader for selective investigations of cell membranes," *J. Biomed. Opt.* **11**, 034011 (2006).
12. T. Nagai and A. Miyawaki, "A high-throughput method for development of FRET-based indicators for proteolysis," *Biochem. Biophys. Res. Commun.* **319**(1), 72–77 (2004).
13. D. V. O'Connor and D. Phillips, *Time-Correlated Single Photon Counting*, Academic Press, London (1984).
14. J. R. Lakowicz, *Principles of Fluorescence Spectroscopy*, Plenum Press, New York (1986).
15. K. Stock, R. Sailer, W. S. L. Strauss, M. Lyttek, R. Steiner, and H. Schneckenburger, "Variable-angle total internal reflection fluorescence microscopy (VA-TIRFM): realization and application of a compact illumination device," *J. Microsc.* **211**, 19–29 (2003).
16. C. G. Coates, D. J. Denvir, N. G. McHale, K. D. Thornbury, and M. A. Hollywood, "Optimizing low-light microscopy with back-illuminated electron multiplying charge-coupled device: enhanced sensitivity, speed and resolution," *J. Biomed. Opt.* **9**(6), 1244–1252 (2004).
17. M. Köhler, S. V. Zaitsev, I. I. Zaitseva, B. Leibiger, I. B. Leibiger, M. Turunen, I. L. Kapelioukh, L. Bakkman, I. B. Appelskog, J. B. de Monvel, G. Imre, and P. O. Berggren, "On-line monitoring of apoptosis in insulin-secreting cells," *Diabetes* **52**(12), 2943–2950 (2003).
18. R. Grailhe, F. Merola, J. Ridard, S. Couvignou, C. LePoupon, J.-P. Changeux, and H. Laguitton-Pasquier, "Monitoring protein interactions in the living cell through the fluorescence decays of the cyan fluorescent proteins," *ChemPhysChem* **7**, 1442–1454 (2006).
19. R. Ramadass, D. Becker, M. Jendrach, and J. Bereiter-Hahn, "Spectrally and spatially resolved fluorescence lifetime imaging in living cells: TRPV4-microfilament interactions," *Arch. Biochem. Biophys.* **463**(1), 27–36 (2007).
20. J. Jones, R. Heim, E. Hare, J. Stack, and B. A. Pollok, "Development and application of a GFP-FRET intracellular caspase assay for drug screening," *J. Biomol. Screening* **5**(5), 307–318 (2000).
21. H. Tian, L. Ip, H. Luo, D. C. Chang, and K. Q. Luo, "A high throughput drug screen based on fluorescence resonance energy transfer (FRET) for anticancer activity of compounds from herbal medicine," *Br. J. Pharmacol.* **150**(3), 321–334 (2007).